

Bobcat-1, the Ohio University CubeSat: preliminary data analysis

Kevin Croissant, Gregory Jenkins, Ryan McKnight, Brian C. Peters,
Sabrina Ugazio and Frank van Graas
Ohio University

BIOGRAPHIES

Kevin Croissant is pursuing his BSEE in Computer Engineering at Ohio University. He is a research intern with the Avionics Engineering Center where his focuses are in particular on software-defined radio for low-frequency time-transfer and development of the Bobcat-1 CubeSat for GNSS Inter-constellation Time-Offset Determination.

Gregory Jenkins is pursuing his MSEE at Ohio University. He is a research intern with the Avionics Engineering Center and is involved with the development of the Bobcat-1 CubeSat for GNSS Inter-constellation Time-Offset Determination.

Ryan McKnight is pursuing his MSEE at Ohio University. He is a research intern with the Avionics Engineering Center and is involved with the development of the Bobcat-1 CubeSat for GNSS Inter-constellation Time-Offset Determination.

Brian C. Peters is pursuing his MSEE at Ohio University. He is a research intern with the Avionics Engineering Center and is involved with the development of the Bobcat-1 CubeSat for GNSS Inter-constellation Time-Offset Determination.

Sabrina Ugazio is an Assistant Professor in Electrical Engineering and Computer Science at Ohio University. She received her Ph.D. in Electronics and Telecommunications Engineering from Politecnico di Torino in 2013. Her research interests include various aspects of GNSS, such as timing, signal monitoring and remote sensing.

Frank van Graas holds an endowed Fritz J. and Dolores H. Russ Professorship in Electrical Engineering and Computer Science, and is a Principal Investigator with the Avionics Engineering Center at Ohio University. Dr. Van Graas is a Past President of The Institute of Navigation (1998–1999) and served as the Institute of Navigation (ION) executive branch fellow at the Space Communications and Navigation Office, National Aeronautics and Space Administration, Washington, DC (2009). He is a fellow of the ION (2001) and received the ION Kepler (1996), Thurlow (2002), and Burka (2010) awards, as well as the American Institute of Aeronautics and Astronautics John Ruth Avionics Award (2010). He has been actively involved with navigation and timing research since 1984.

ABSTRACT

Bobcat-1 is a 3-unit CubeSat developed at Ohio University's Avionics Engineering Center within the Russ College of Engineering and Technology. It was selected for launch through the NASA CubeSat Launch Initiative (CSLI) and manifested for flight on Educational Launch of Nanosatellites (ElaNa) Mission 31, which launched on October 2, 2020. Bobcat-1 was deployed from the ISS on November 5, 2020. After deployment, the CubeSat started collecting GNSS data which has been downlinked to the ground station at Ohio University. In this paper, the preliminary results from the processing of the collected data from space will be presented. The main scientific objective of the Bobcat-1 mission is to evaluate the performance of inter-constellation time offset estimates from Low Earth Orbit (LEO). The primary payload on Bobcat-1 is a multi-frequency, multi-constellation NovAtel OEM-719 GNSS receiver, which tracks satellites from GPS, Galileo, GLONASS, BeiDou and QZSS. The main benefits of a GNSS receiver at LEO is the possibility to obtain data from multiple satellites multiple times a day: given the low orbit (~400 km) and the short orbit period (~90 minutes), the lack of troposphere delay errors, and the low multipath environment. In this paper, the operational status and measurement quality analysis will be presented, including spectrum observations, carrier-to-noise ratio, and solution residuals.

INTRODUCTION

Bobcat-1, shown in Figure 1, is a 3-unit nanosatellite (a CubeSat constituted of 3 units) developed at Ohio University's Avionics Engineering Center within the Russ College of Engineering and Technology. In this section, Bobcat-1's primary mission objective is described, including the motivations of the work, as well as an overview on the mission and the main payload. More details are provided in [1, 2].

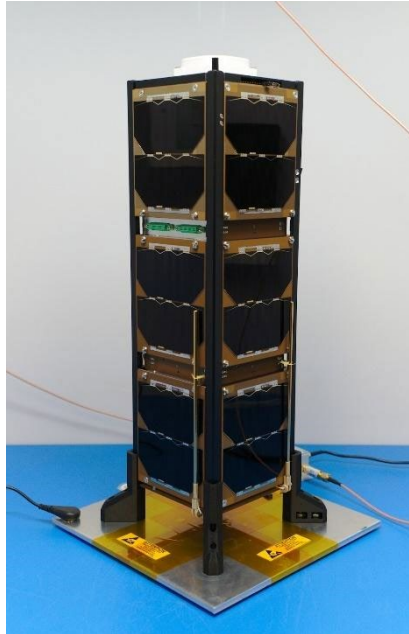


Figure 1. Bobcat-1 in the clean box at the Ohio University's Avionics Engineering Center, during the last phases of testing before deployment. In this image, the communication antenna is not deployed.

Bobcat-1 was selected for launch through the NASA CubeSat Launch Initiative (CSLI) [3] and manifested for flight on Educational Launch of Nanosatellites (ElaNa) Mission 31, which launched on October 2, 2020. Bobcat-1 was deployed from the International Space Station (ISS) on November 5, 2020; after deployment, Bobcat-1 started collecting data, which has been downlinked to the ground station at Ohio University for post-processing analysis. Details on Bobcat-1 design and mission planning are provided in [3].

Bobcat-1's primary mission goal is to evaluate the performance of Global Navigation Satellite System (GNSS) inter-constellation time offset estimates from Low Earth Orbit (LEO).

Each GNSS system is synchronized to an independent time reference. As a consequence, inter-constellation time offsets are present between each system, and represent an additional unknown in a multi-GNSS solution, i.e., when solving for a user's PVT using satellites from multiple constellations. The presence of unknown inter-constellation time offset may represent a limit to the solution availability and accuracy for users with limited visibility due to a challenging environment (e.g., urban canyon [4]). Those users could benefit, improving their GNSS solution both in terms of availability and accuracy, if provided with inter-constellation time offset estimates from an external source. The target users are the high-altitude Space Service Volume (SSV), such as Geostationary Orbit (GEO) satellites [5-7].

Different methods for inter-constellation time offsets estimates have been proposed and implemented; worldwide networks of receivers are currently utilized to mitigate the biases due to the estimating receiver and between the same-constellation satellites [8,9]. Bobcat-1 enables the experimental estimation of GNSS inter-constellation time offsets from LEO, exploiting key advantages enabled by the low earth orbit environment, and by the small dimension of the CubeSat: the relatively short orbit period allows for the visibility of a high number of GNSS satellites, multiple times per day (Bobcat-1 performs about 15 orbits per day). Moreover, the GNSS receiver on Bobcat-1 experiences no tropospheric error, and low multipath error. Bobcat-1 is currently collecting GNSS data and downlinking them to the ground station, for post-processing.

The primary payload on Bobcat-1 is a multi-constellation, multi-frequency, NovAtel OEM-719 GNSS receiver, shown in Figure 2, capable of tracking signals from GPS, Galileo, GLONASS, BeiDou and QZSS, at different frequencies. The NovAtel OEM-719 receiver supports a wide variety of signals, as summarized in Table 1. In this paper, an analysis of spectrum observations, carrier-to-noise ratio, and solution residuals will be presented, to provide an evaluation of the measurements' quality.



Figure 2. Novatel OEM719 GNSS receiver.

Table 1. NovAtel OEM-719 supported signals.

GNSS constellation	Supported signals
GPS	L1 C/A, L1C, L2C, L2P, L5
GLONASS	L1, L2, L3, L5
BeiDou	B1, B2, B3
Galileo	E1, E5 AltBOC, E5a, E5b, E6
IRNSS	L5
SBAS	L1, L5

DEPLOYMENT

Bobcat-1 was launched on October 2nd, 2020 aboard Cygnus NG-14, from NASA Wallops Flight Facility (Figure 3) as part of the ELaNa 31 mission, alongside 2 other university CubeSats:

- NEUTRON-1 - University of Hawaii-Mānoa;
- SPOC - University of Georgia.

Bobcat-1 was deployed on November 5th, 09:05 UTC from the International Space Station via Nanoracks CubeSat Deployer (Figure 4), with an initial orbit altitude of about 408 km above sea level. The expected life-span of the CubeSat is about six months.



Figure 3. ELaNa 31 mission launch, with Bobcat-1 on board of Cygnus NG-14.

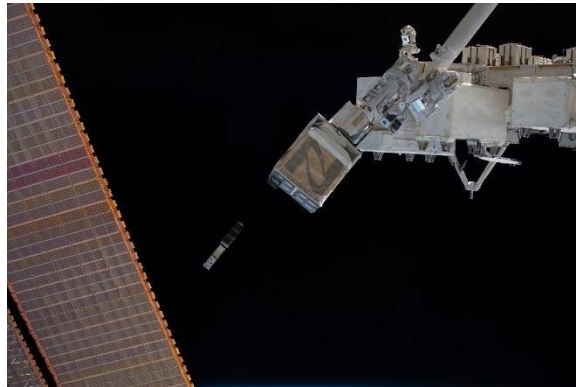


Figure 4. Bobcat-1 deployment from ISS.
Credit: NASA

OPERATIONAL STATUS

To date, 26 data collections completed and downlinked supporting Bobcat-1's mission goals comprising a total of 238MB of data. The CubeSats in-orbit power budget has closely matched the preliminary design model, which has enabled continuous data collections for multiple consecutive orbits. Figures 5 and 6, taken from Bobcat-1's telemetry dashboard, show the CubeSat's solar power generated per face and the battery input/output power. The data shown is recorded as the satellite emerged from eclipse over the ground station at Ohio University, 2020-12-29 6:53 AM EST.

Figure 7 displays the battery input and output power during a data collection on the CubeSat. The power draw exceeds the amount that can be generated when the NovAtel receiver is powered on, which results in the battery slowly draining over multiple orbits. Typically, data collections are limited by the amount of flash storage available on Bobcat-1's onboard computer more than they are by the power budget. Data collections are configured to automatically end if the flash storage becomes full, or if the battery voltage drops below a certain threshold.

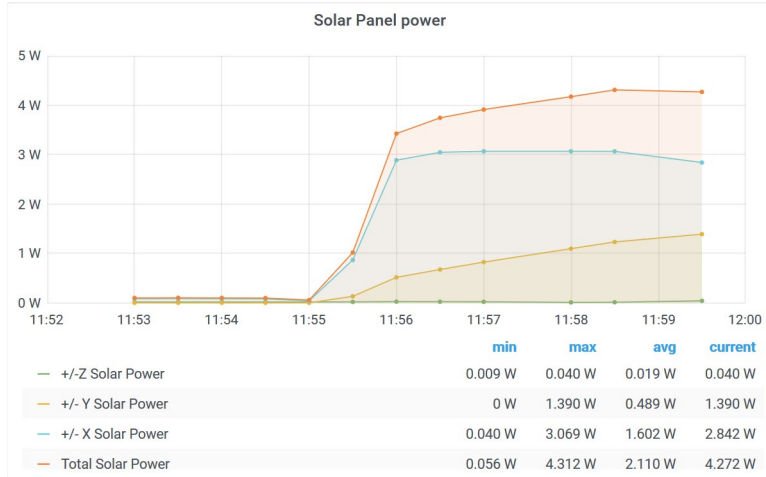


Figure 5. Bobcat-1 Solar Panel Power

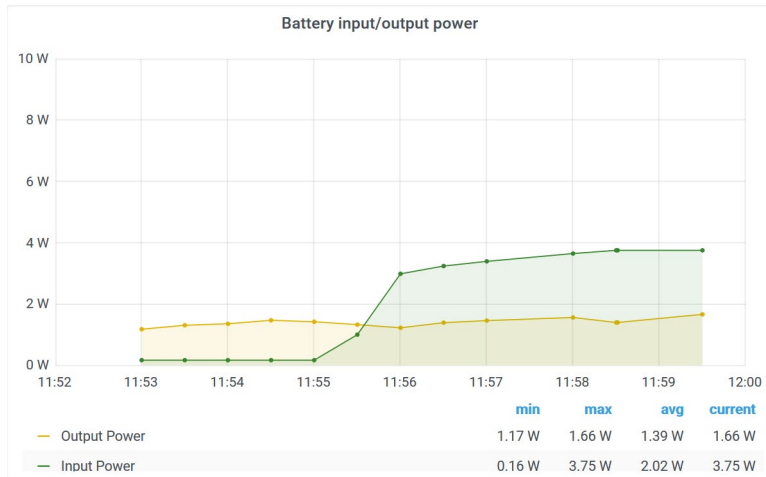


Figure 6. Battery Input/Output Power (CubeSat Idle)

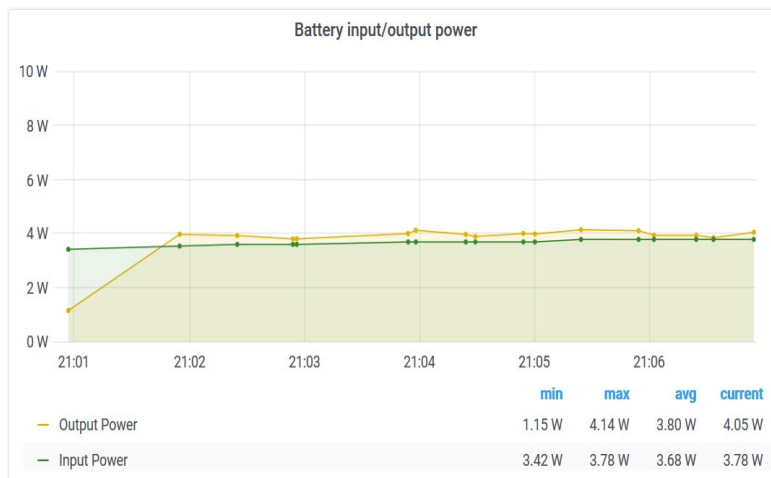


Figure 7. Battery Input/Output Power (Data Collection)

Bobcat-1 telemetry is received and decoded worldwide by the SatNOGS network of amateur radio ground stations. Most SatNOGS ground stations use low-cost software-defined radios and GNURadio flowgraphs to demodulate telemetry beacons. Beacons are also decoded manually by amateur radio operators using conventional hardware radios and soundcard modems. All of Bobcat-1’s housekeeping data is shared publicly in real-time on a public data dashboard¹ hosted by SatNOGS. As of 2021-02-04, 120 stations have contributed decoded beacons to Bobcat-1’s telemetry dashboard.

PRELIMINARY DATA ANALYSIS

The first step in ensuring a clean measurement environment is to evaluate the spectrum around the frequency band of interest. To collect spectrum data, the CubeSat was programmed to collect spectrum bursts approximately five times per orbit. For this experiment, each spectrum measurement provides the power in 204 spectrum bins with a width of 488 kHz each. The start frequency is 1531.5 MHz and the stop frequency is 1630.6 MHz for a bandwidth of approximately 100 MHz. For thermal noise only, the power in each bin should be approximately -117 dBm, which matches the measurement example provided in Figure 8. This measurement was taken by the calibrated OEM-719 receiver when the CubeSat flew close to the US East Coast on November 21, 2020 at 22:18 UTC. To reduce the noise on the spectrum, 20 successive measurements spaced by 1 second were averaged for each of the 204 bins. In the spectrum, a 2-3 dB peak can be observed around the GPS L1 frequency of 1575.42 MHz. This peak represents the combined power of all visible satellites at the L1 frequency. Although each individual satellite is below the noise floor, the combined power exceeds the noise floor by a few dB. From Figure 8, it can be concluded that the CubeSat spectrum environment is clean; no spurious transmissions are present that could degrade the measurement quality.

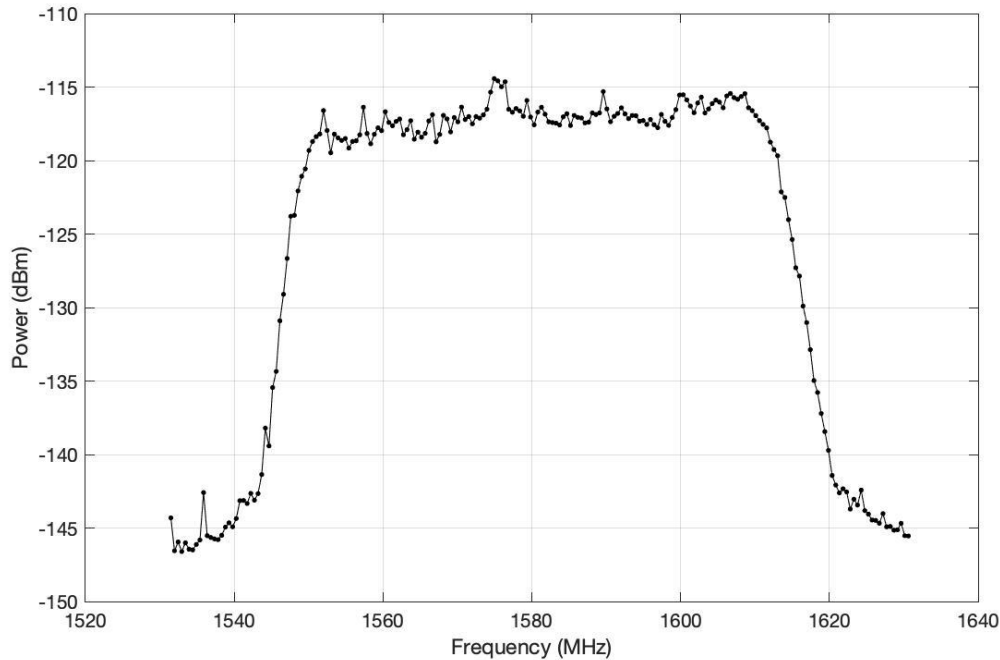


Figure 8. Average Power Spectral Density for 20 Measurements

The spectrum measurements were translated into a Jamming to Signal ratio (J/S) in a 20-MHz bandwidth with respect to the P(Y) code minimum signal power reference of -133 dBm. The power in the 20-MHz GPS band around L1 is obtained by summing the power from the 40 spectrum bins in Figure 8, centered around L1. In the presence of noise only, the J/S calculation results in:

$$J/S = 10 \log_{10} \left(\frac{\sum_{i=1}^{40} P_i}{10^{-13.3}} \right) = 10 \log_{10} \left(\frac{40 \times (10^{-11.7})}{10^{-13.3}} \right) \approx 32 \text{ dB} \quad (1)$$

The J/S levels were plotted on a world map along with the ground track of the CubeSat (in yellow) for approximately one orbit on November 21, 2020. The orbit started at 22:18 close to the US East Coast and ended at 23:30 UTC. Green dots indicate a

¹ <https://dashboard.satnogs.org/>

J/S below 33 dB, while red indicates a J/S above 35 dB. From Figure 9, it is observed that J/S above 35 dB was experienced while flying over South-East Europe. For the purpose of the CubeSat’s primary mission, measurements collected in the presence of interference will not be used for the estimation of inter-constellation time offsets.

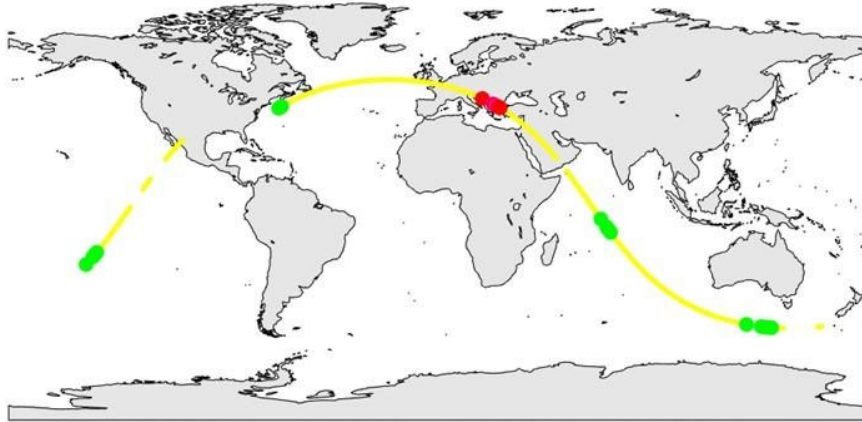


Figure 9. Worldwide Spectrum Snapshots Translated to Jamming to Signal Ratio (J/S) for GPS L1 in a 20-MHz Bandwidth. Yellow Represents the CubeSat Ground Track, Green Represents a J/S < 33 dB, Red Represents a J/S > 35 dB

A Code-Minus-Carrier (CMC) analysis was performed to evaluate the presence of multipath and antenna group delay error variations in the CubeSat GPS measurements. A CMC observable is the difference between the pseudorange and the carrier phase measurements corrected for ionosphere delay variation. Also, the mean value of the CMC over one satellite track is subtracted from the CMC. CMC cancels all errors except for [10]:

- Pseudorange thermal noise
- Pseudorange multipath
- Antenna group delay variations
- Residual filtering errors due to dynamics (e.g. fast ionosphere changes)
- Carrier phase thermal noise
- Carrier phase multipath
- Antenna phase delay variations
- Phase wrap-up

The ionospheric delay variations for the L1 frequency are calculated using:

$$\Delta I_{L1}(t) = \frac{f_{L2}^2}{f_{L2}^2 - f_{L1}^2} (\phi_{L2}(t) - \phi_{L1}(t)) \tag{2}$$

where ϕ_{L1} and ϕ_{L2} are the integrated carrier phases at the L1 and L2 frequencies, respectively.

The pseudorange thermal noise is expected to be at the 5 to 10 cm-level (rms), carrier phase thermal noise should be less than 1 mm (rms). Carrier phase multipath should be below 1 cm, antenna phase delay variations are at the mm-level, and antenna phase wrap-up after correction should be below a few cm. Residual filtering errors due to dynamics are minimized by using L2C for the dual-frequency ionospheric delay variation correction. In addition, satellites are selected based on the following criteria:

- Satellites must be received in the primary beam pattern of the CubeSat GNSS antenna, which is determined by a C/N₀ measurement above 40 dB-Hz
- Ionospheric delay variations must be small or slowly varying as indicated by the dual frequency carrier phase-based correction
- Satellites must be above five degrees with respect to the local CubeSat horizon

In summary, the CMC should be dominated by pseudorange thermal noise, pseudorange multipath, and antenna group delay variations. Due to the wideband design of the GNSS antenna, antenna group delay variation errors are expected to be below 10

cm [11], while pseudorange multipath errors should also be below 10 cm due to the small size of the CubeSat. To illustrate the CMC performance of the CubeSat measurements, three satellites were selected for a detailed analysis of CMC, using data from a CubeSat orbit on December 23, 2020. Figure 10 through Figure 12 show the results for PRN 3, 5, and 8, respectively. The top plot in each figure is the CMC and shows high-precision measurement performance with standard deviations of 0.12, 0.09, and 0.11 m, respectively, for measurement updates every 5 s. The middle plot in each figure shows the C/N_0 for both L1 (in blue) and L2 (in red). The peak values reach around 50 dB-Hz, which indicates no significant implementation losses in the front-end design. Also of note is the smoothness of the curves confirming the absence of high-frequency multipath. The bottom plot in each figure shows the L1 frequency ionosphere delay variation calculated using Equation (2). This measurement only uses the carrier phase from the GPS L1 and L2 frequencies and also shows a smooth pattern, indicating that no high-frequency contents are present that could induce errors on the pseudorange measurements through the receiver's carrier aiding of the code tracking loop.

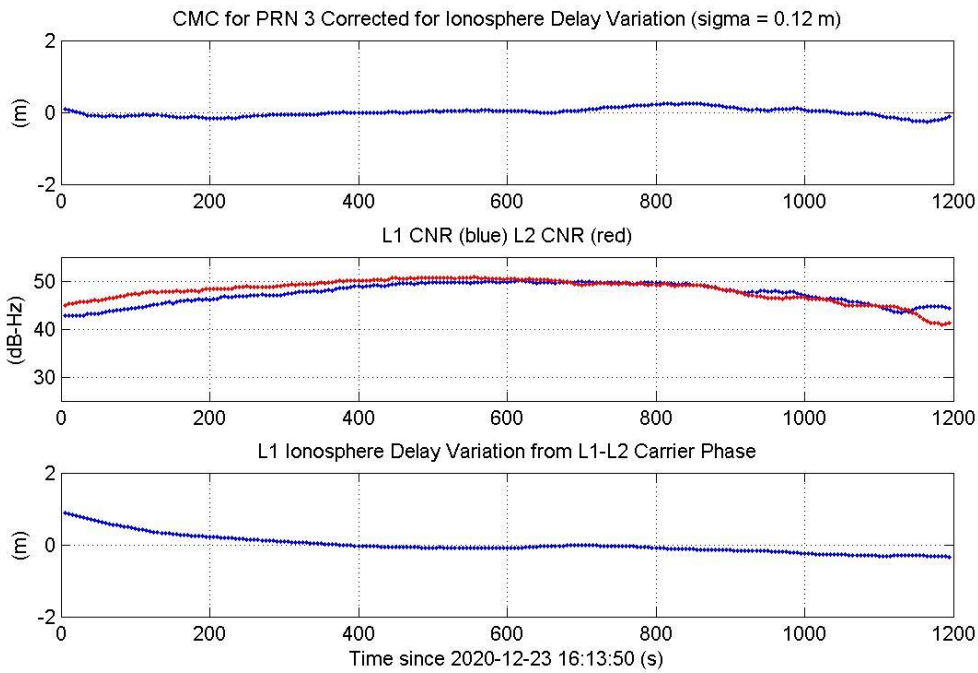


Figure 10. Code-Minus-Carrier for PRN 3 (top), Carrier-to-Noise Ratio (middle), Ionosphere Delay Variation (bottom)

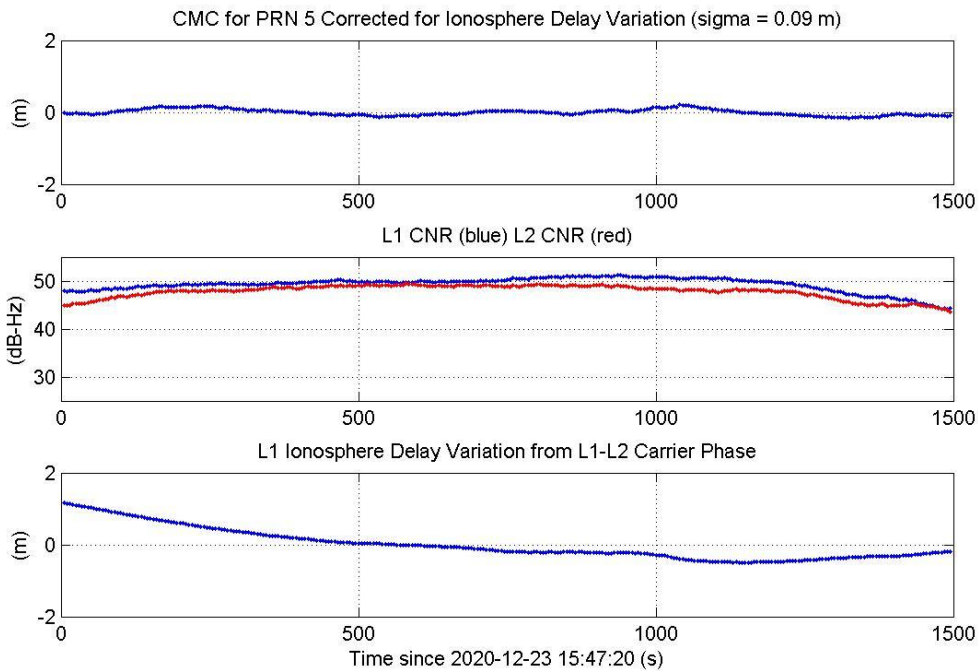


Figure 11. Code-Minus-Carrier for PRN 5 (top), Carrier-to-Noise Ratio (middle), Ionosphere Delay Variation (bottom)

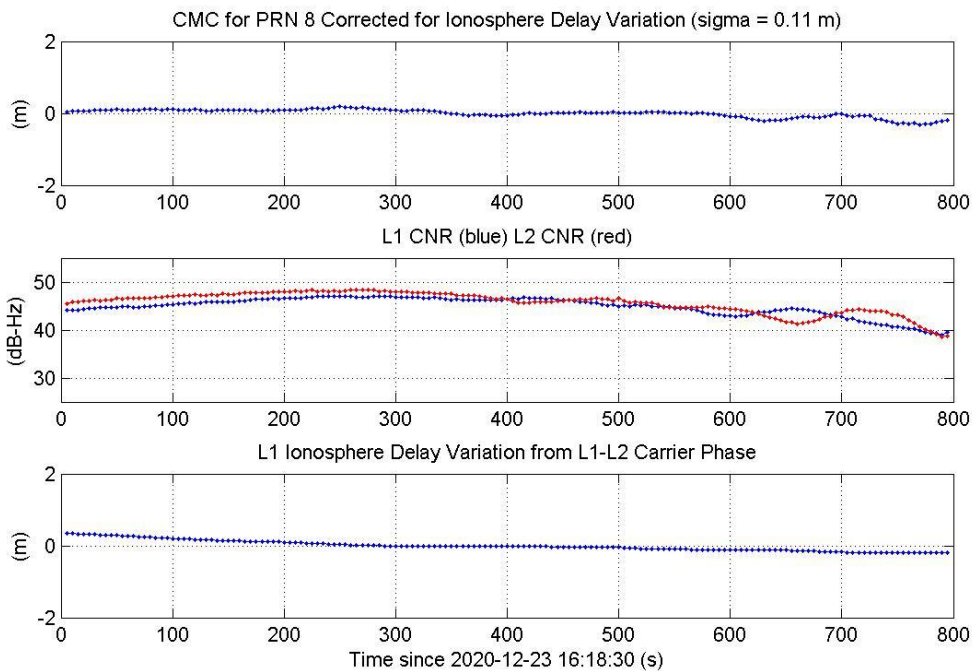


Figure 12. Code-Minus-Carrier for PRN 8 (top), Carrier-to-Noise Ratio (middle), Ionosphere Delay Variation (bottom)

It can be concluded that the CMC analysis demonstrates high measurement quality for the GPS L1 pseudorange measurements with noise around 0.1 m (1-sigma) and very smooth C/N_0 and ionosphere delay variation corrections. The CMC standard deviations are summarized in Table 2.

Table 2. Summary of CMC Performance

PRN	CMC Standard Deviation
3	0.12 m
5	0.09 m
8	0.11 m

To characterize the antenna group delay and multipath performance outside the main antenna pattern, PRN 27 was selected with C/N_0 varying around 40 dB-Hz for both the L1 and L2 frequencies as shown in Figure 13. Ionosphere delay variation was confirmed to be small in the bottom plot of Figure 13, such that the CMC is a good indicator of the antenna performance for signals that arrive below the local antenna horizon. For this case, CMC errors up to -1 m were observed with a standard deviation of 0.32 m. Most likely, these variations are caused by the relatively small, square ground plane and interaction of the antenna with the 3-U structure below the antenna ground plane. The ground plane is 10 by 10 cm, while the antenna is 5 by 5 cm. Since the errors are relatively small with a smooth structure, we are planning to map these errors using a “tumbling” motion of the CubeSat, similar to terrestrial techniques used to measure antenna group delay variations using a rotator, see, for example [11].

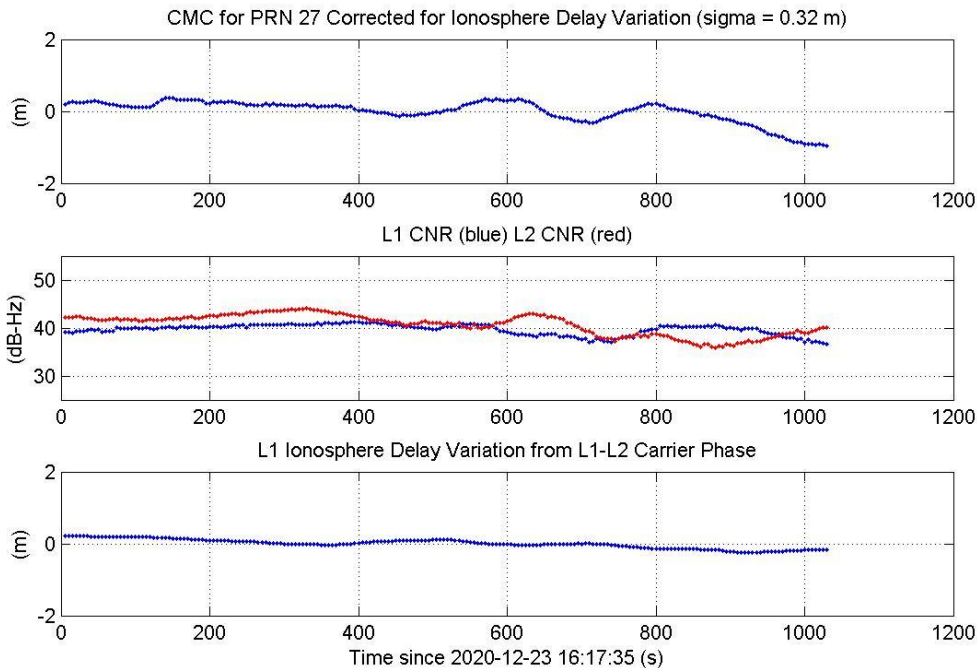


Figure 13. Code-Minus-Carrier for PRN 27 (top), Carrier-to-Noise Ratio (middle), Ionosphere Delay Variation (bottom)

For a preliminary evaluation of the positioning performance, the same data set used for the CMC analysis was also used for a visibility and residual analysis. Figure 14 shows the CubeSat ground track on December 23, 2020 for one orbit that started at 15:26:20 and ended at 16:59:55 UTC. The black dot indicates the start of the orbit. In the right plot of Figure 14, the skyplot is shown that has the track of each of the GPS satellites during the orbit with respect to the local CubeSat horizon. The outer ring in this plot is the local horizon, while the middle of the plot is the zenith direction at the CubeSat location. Therefore, the skyplot shows the track of each of the GPS satellites in the sky relative to the CubeSat. During a single 90-minute orbit, the CubeSat is able to obtain measurements from all GPS satellites. The skyplot also demonstrates excellent tracking performance of the OEM-719 GNSS receiver. Although only satellites above the local CubeSat horizon are shown in the skyplot, the receiver tracks GNSS satellites down to negative 20 deg with respect to the local CubeSat horizon.

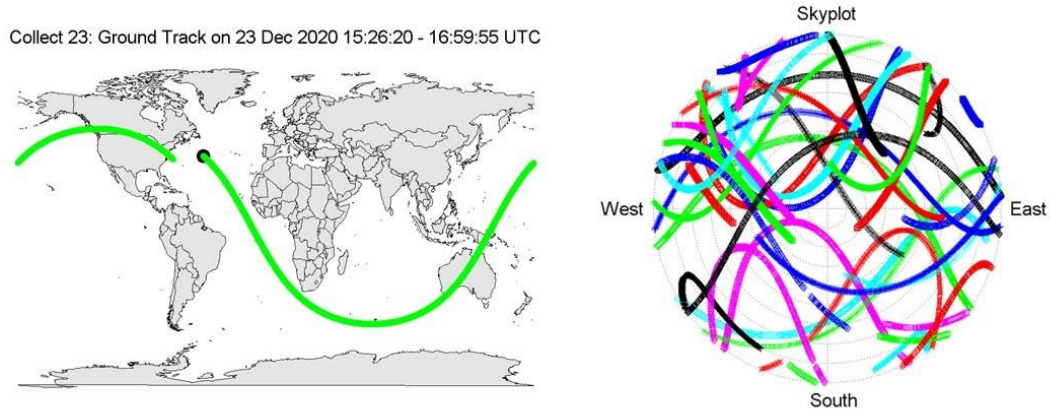


Figure 14. Ground Track for Collect 23 on December 23, 2020 (left), and Satellite Sky Plot (right)

Positioning performance was evaluated using all GPS satellites that are at least 5 degrees above the local CubeSat horizon. An unweighted least squares solution was used based on GPS L1 C/A code measurements without ionosphere delay corrections. Figure 15 shows the number of visible satellites (in blue) and the position residual (in red). The number of visible satellites varied between 7 and 12 during the orbit. The position residuals varied between 0.4 and 3.3 m with an average value of 1.8 m. Given the average number of visible satellites of approximately 9, the solution residuals are a good indicator of the position accuracy, which is likely at 1-2 m (3D rms). Further improvements are anticipated after the application of ionosphere delay corrections as well as GPS satellite clock and orbit corrections.

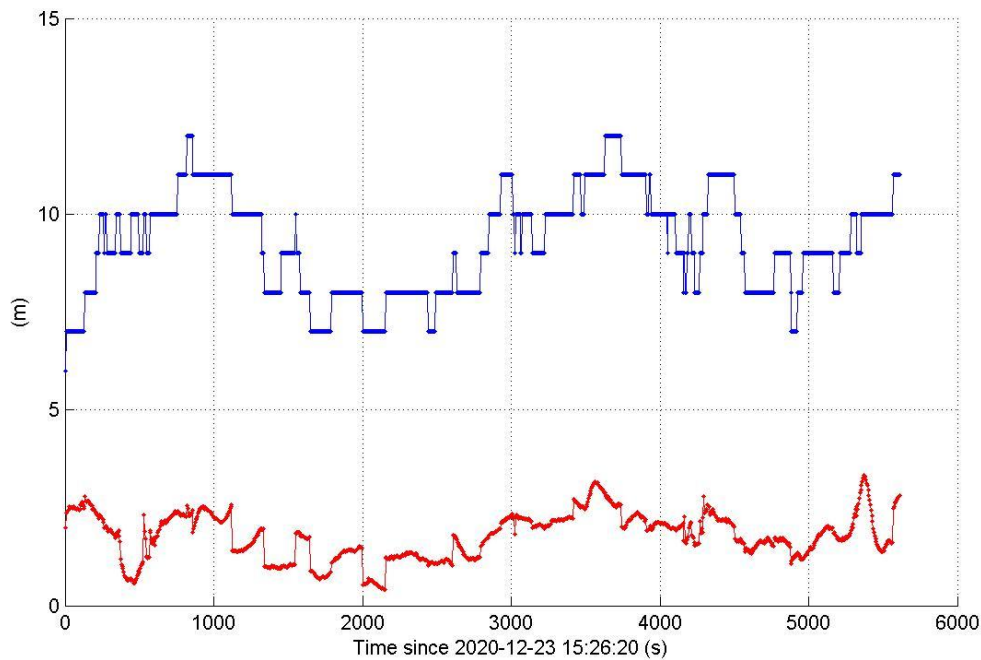


Figure 15. Position residuals (red) and Number of Satellites (blue) for a Mask Angle of 5 deg

CONCLUSIONS AND FUTURE WORK

Following deployment from the ISS on November 5, 2020, all components of Bobcat-1 have been demonstrated to be fully operational. GPS measurement precision for the L1 C/A code is approximately 0.1 m (rms) based on a Code-Minus-Carrier (CMC) analysis of several GPS satellites. This level of performance indicates that the multipath and antenna group delay

variation errors combined with thermal noise are well within our accuracy budget of 0.3 m needed for ns-level estimation of inter-constellation time offsets.

Future work will be focused on the application of precise GNSS clock and orbit corrections, ionosphere delay corrections, and temperature-dependent hardware delay corrections. The solution will be expanded to include additional constellations and to estimate the time offsets between the constellations.

ACKNOWLEDGMENTS

The authors would like to acknowledge the NASA CubeSat Launch Initiative, NASA Glenn Research Center and Ohio University for sponsoring the Bobcat-1 project.

REFERENCES

1. Ugazio, Sabrina, Peters, Brian C., Croissant, Kevin, Jenkins, Gregory, McKnight, Ryan, van Graas, Frank, "GNSS Inter-system Time-Offset Estimates and Impact on High Altitude SSV," Proceedings of the 2020 International Technical Meeting of The Institute of Navigation, San Diego, California, January 2020, pp. 320-330.
2. Croissant, Kevin, Jenkins, Gregory, McKnight, Ryan, Peters, Brian C., Ugazio, Sabrina, van Graas, Frank, "Design and mission planning of Bobcat-1, the Ohio University CubeSat," *Proceedings of the 33rd International Technical Meeting of the Satellite Division of The Institute of Navigation (ION GNSS+ 2020)*, , September 2020, pp. 1383-1393.
3. "CubeSat101: Basic Concepts and Processes for First-Time CubeSat Developers", https://www.nasa.gov/sites/default/files/atoms/files/nasa_csl_i_cubesat_101_508.pdf
4. Melman, Floor Thomas, Rodriguez, Rafael Lucas, Villamide, Xurxo Otero, Swinden, Richard, Crosta, Paolo, Galluzzo, Gaetano, "Using Broadcast Time Offsets for Multi-Constellation Users in Harsh Environments," Proceedings of the 51st Annual Precise Time and Time Interval Systems and Applications Meeting, San Diego, California, January 2020, pp. 267-278.
5. Bauer, F. H., "GPS Space Service Volume (SSV) Ensuring Consistent Utility Across GPS Design Builds for Space Users", Presented at the 15th PNT Advisory Board Meeting, June 11, 2015.
6. Parker, Joel J. K., Bauer, Frank H., Ashman, Benjamin W., Miller, James J., Enderle, Werner, Blonski, Daniel, "Development of an Interoperable GNSS Space Service Volume," Proceedings of the 31st International Technical Meeting of The Satellite Division of the Institute of Navigation (ION GNSS+ 2018), Miami, Florida, September 2018, pp. 1246-1256.
7. "NASA Proposed Updates to ICG SSV Booklet", 11 June 2019 Vienna, Austria UN ICG WG-B Space Users Subgroup Meeting Joel J. K. Parker, Frank H. Bauer, James J. Miller
8. Montenbruck O. et al (2017) The Multi-GNSS experiment (MGEX) of the international GNSS service (IGS)—achievements, prospects and challenges. *Adv Space Res* 59(7):1671–1697. <https://doi.org/10.1016/j.asr.2017.01.011>
9. Oliver Montenbruck, Peter Steigenberger, Lars Prange, Zhiguo Deng, Qile Zhao, Felix Perosanz, Ignacio Romero, Carey Noll, Andrea Stürze, Georg Weber, Ralf Schmid, Ken MacLeod, Stefan Schaer, The Multi-GNSS Experiment (MGEX) of the International GNSS Service (IGS) – Achievements, prospects and challenges, *Advances in Space Research*, Volume 59, Issue 7, 1 April 2017, Pages 1671-1697, ISSN 0273-1177, <http://dx.doi.org/10.1016/j.asr.2017.01.011>.
10. Van Graas, F., Bartone, C., Arthur, T., "GPS Antenna Phase and Group Delay Corrections," Proceedings of the 2004 National Technical Meeting of The Institute of Navigation, San Diego, CA, January 2004, pp. 399-408.
11. Raghuvanshi, A., Van Graas, F., "Characterization of Airborne Antenna Group Delay Biases as a Function of Arrival Angle for Aircraft Precision Approach Operations," Proceedings of the 28th International Technical Meeting of the Satellite Division of The Institute of Navigation (ION GNSS+ 2015), Tampa, Florida, September 2015, pp. 3681-3686.